

# Crystallographic Properties and Surface Analysis of Spin Coated YSZ Thin Films by Raman Spectroscopy, X-ray Diffraction and Scanning Electron Microscopy

Shirley Tiong Palisoc, Simon Gerard Mendiola, Rose Ann Tegio, Michelle Natividad, Kevin Kaw, Stephen Tadios, Benjamin Tuason

**Abstract**— Yttria Stabilized Zirconia (YSZ) thin films (<10  $\mu\text{m}$ ) were fabricated by spin coating technique on steel (Fe/ Cr18/ Ni10). The concentration ratio of YSZ powder to solvent were varied accordingly. The effects of these variations were investigated and discussed. Using X-ray Diffraction and Raman Spectroscopy, the crystal structure of the samples were determined. The 8-YSZ thin films have cubic fluorite structure. The X-ray diffraction patterns were in agreement with the samples' Raman spectra. In the case of the 30<sub>YSZ</sub>: 70<sub>ethanol</sub> YSZ thin film on steel substrate, the Raman and XRD peaks shifted because of the stress-strain interaction between the steel and the YSZ thin film. Pores were evident on single coated substrates but were minimized using higher YSZ concentrations.

**Index Terms**— Yttria Stabilized Zirconia, YSZ, spin-coating, thin film

## 1 INTRODUCTION

In order to answer the need for alternative sources of energy and to stop the effects of global warming, many researches and studies have risen, one of which is that on Solid Oxide Fuel Cells (SOFCs). A Solid Oxide Fuel Cell (SOFC) is an energy-converting device or electrochemical power generation device, which can directly generate electricity from chemical energy.<sup>1-3</sup> It can generate electricity at a high efficiency and in an environmentally friendly way. The commonly used material for the electrolyte of SOFC is Yttria-stabilized zirconia (YSZ) because it can work at high temperatures in a highly efficient way.<sup>4</sup> Furthermore, YSZ is readily available and is a good ion conductor.

Currently, conventional SOFCs operate at high temperatures (800°C -1000°C).<sup>5</sup> The high operating temperature is necessary to obtain the maximum efficiency but as a consequence, it can cause reactions and interdiffusion in the cell especially in a long-term operation. As a result, it will reduce cell performance and efficiency.<sup>6</sup>

In order to avoid the unnecessary reactions and complications, the current demand for the development of SOFC is to de-

crease the operational temperature to the range of 600°C - 800°C (Intermediate Temperature SOFC or IT-SOFC).<sup>5</sup> To be able to comply with the new operational temperature range and improve its operational life, it is necessary to decrease the electrolyte resistance and lower the overpotential of the electrodes.<sup>2</sup> The necessary adjustments can be done through decreasing the thickness of the electrolyte which should be less than 1 $\mu\text{m}$ .

Numerous techniques can be used in order to make a thin electrolyte. This includes chemical and physical deposition, such as electrochemical vapor deposition or magnetron sputtering, and liquid precursor and powder processing techniques such as spin coating, die pressing.<sup>4-7</sup> The aforementioned techniques except for spin coating are very costly and insurmountable to do because these techniques require a lot of training and cost-inefficient. At the given time frame, the only method that can be easily executed is the spin coating technique which is the least complicated and cost-effective.

## 2 METHODS

### 2.1. Preparation of the YSZ thin film

8-YSZ ((Y<sub>2</sub>O<sub>3</sub>)<sub>0.08</sub> (ZrO<sub>2</sub>)<sub>0.92</sub>) thin films were fabricated using the spin coating technique. Commercially available 8-YSZ powder (fuelcelmaterials, particle size: <1 $\mu\text{m}$ , purity: 99.9%) was diluted in ethanol (Figure 8b) (Aced Laboratory, purity: 95%) in order to make a suspension. The suspension was then homogenized using the ultrasonic stirrer for 3 hours. This homogenizing process was done in all sample concentrations, specifically, 10<sub>YSZ</sub>:90<sub>ethanol</sub>, 30<sub>YSZ</sub>:70<sub>ethanol</sub> and 50<sub>YSZ</sub>:50<sub>ethanol</sub>. (Note: the YSZ and ethanol ratio is expressed in weight percent)

The substrate underwent two coating stages. The first coating stage had a rotation speed of 700rpm for 6 seconds and the second cycle had a rotation speed of 2400-2500 rpm for 25-30 seconds.

- Shirley Tiong Palisoc Ph.D. In Materials Science is a professor at the Department of Physics, De La Salle University – Manila, Philippines. E-mail: shirley.palisoc@dlsu.edu.ph
- Simon Gerard Mendiola is a test engineer at Hitachi Philippines. E-mail: sg\_mendiola@yahoo.com
- Rose Ann Tegio is a junior officer at PNB – Manila, Philippines.
- Michelle Natividad Ph.D. in Physics is an assistant professor at the Department of Physics, De La Salle University – Manila, Philippines. E-mail: michelle.natividad@dlsu.edu.ph
- Kevin Kaw is a senior student at De La Salle University – Manila, Philippines. E-mail: kevinkaw08@yahoo.com
- Stephen Tadios is a senior student at De La Salle University – Manila, Philippines. E-mail: stephentadios@yahoo.com
- Benjamin Tuason is a senior student at De La Salle University – Manila, Philippines. E-Mail: benjamintuason@yahoo.com

The coated substrate was baked in a furnace at 300°C for 3 minutes to remove excess moisture. Then the coated substrate was sintered in a furnace at about 650°C for 4 hours with a heating and cooling rate of 2C°/min.

### 2.2. Characterization of YSZ thin films

The morphology and cross-section of the sintered samples were studied under the scanning electron microscope (SEM) (JEOL- 5310). Crystal structure and phase change identification of the pre-sintered and sintered samples were studied through x-ray diffraction (with Scan range: 27°-83°, Step size: 0.02 °, Time per step: 0.5s with Cu-K $\alpha$  radiation,  $\lambda=1.541\text{\AA}$  as the parameters). Crystallite size was measured and estimated. The pre-sintered and sintered samples were also characterized by Raman spectroscopic technique using Raman Systems R-3000 (785nm and laser power ~290mW)

## 3 RESULTS

### 3.1. XRD results

Figures 1 to 3 show the same diffraction angles for pre-sintered and sintered samples. This shows that the YSZ is very ideal to be used as a primary electrolyte material since there were no evident phase changes (i.e. appearance of new peaks or doubling of peaks) seen in the pre-sintered and sintered samples. If there was phase change this would greatly affect the performance of the electrolyte because the crystal structure of the electrolyte would be constantly subjected to phase change while operating.

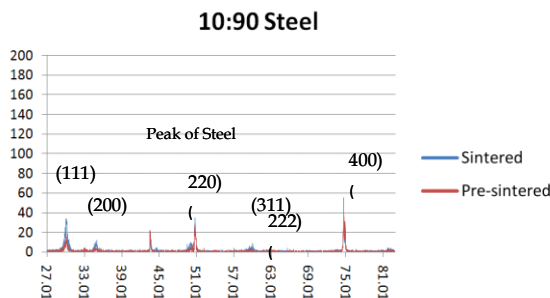


Fig.1 XRD results of 10<sub>YSZ</sub>:90<sub>Ethanol</sub> weight percent ratio on silicon (Si) substrate for pre-sintered (red) and sintered (blue) samples.

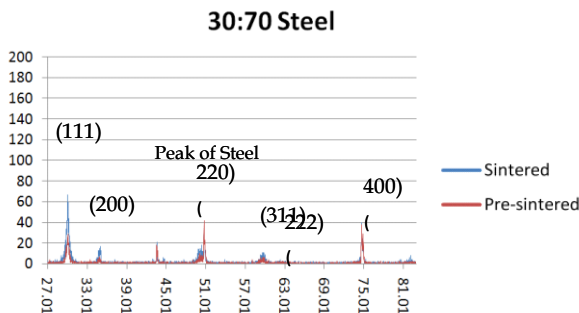


Fig.2 XRD results of 30<sub>YSZ</sub>:70<sub>Ethanol</sub> weight percent ratio on silicon (Si) substrate for pre-sintered (red) and sintered (blue) samples.

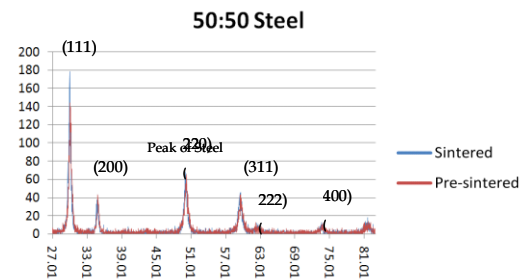


Fig.3 XRD results of 50<sub>YSZ</sub>:50<sub>Ethanol</sub> weight percent ratio on silicon (Si) substrate for pre-sintered (red) and sintered (blue) samples.

All diffraction patterns for both Figures (2 & 3) have similar location (in  $2\theta$ ) of peaks approximately at 30° (111), 35° (200), 50° (220), 59° (311), 63° (222) and 74° (400). Notice also that some peaks in Figure 1-3 (but more prominent in Figure 1 and 2) shifted by a fraction. This shifting can be attributed to the stress and strain at the interface with the steel substrate on the YSZ.

Comparing the intensity of diffraction peaks of Figure 1 to Figure 3, it is evident that the peaks of the sintered samples are higher. This increase of intensity means that larger crystals are present. Since the intensity increases, the width of the peak narrows.

### 3.2 Raman results

Raman spectroscopy was used in order to confirm the results of the XRD. Since this technique is much more sensitive it would confirm that there are other phases (i.e. tetragonal or monoclinic) of YSZ existing in the film. According to the results, the Raman peaks of all samples were consistent all throughout. The first set of peaks ranging from 370/cm to 750/cm were obtained, which showed a good fit with the results of A. Gosh et. al. <sup>9)</sup>

But since the Raman results obtained in this research has a wider scan range, a second set of peaks appeared at range of 1200/cm to 1550/cm. Both sets of peaks are attributed to YSZ and not to any impurity that may be present. As can be seen from Fig. 4 to 6, the peaks in the pre sintered and sintered samples have the similar peak position (wavenumber  $\text{cm}^{-1}$ ). The peaks in the sintered samples are higher and more defined. This affirms the XRD results where sintering alleviates the level of crystallization. Furthermore, as the intensity of the Raman peak increased, the width of the peak decreased as well. This is additional evidence that the YSZ crystal size became larger (better quality).

Figures 4 to 6 indicate that the type of substrate is not a factor in the position of the Raman peaks. There was little or no shift in the Raman peaks as the substrate was changed.

### 3.3 SEM results

#### Surface Analysis

Figure 7 shows the SEM micrographs of sintered steel (Fe/Cr 18/ Ni 10). In Figure 7(a) it can be observed that there are no uneven heavy depositions seen.

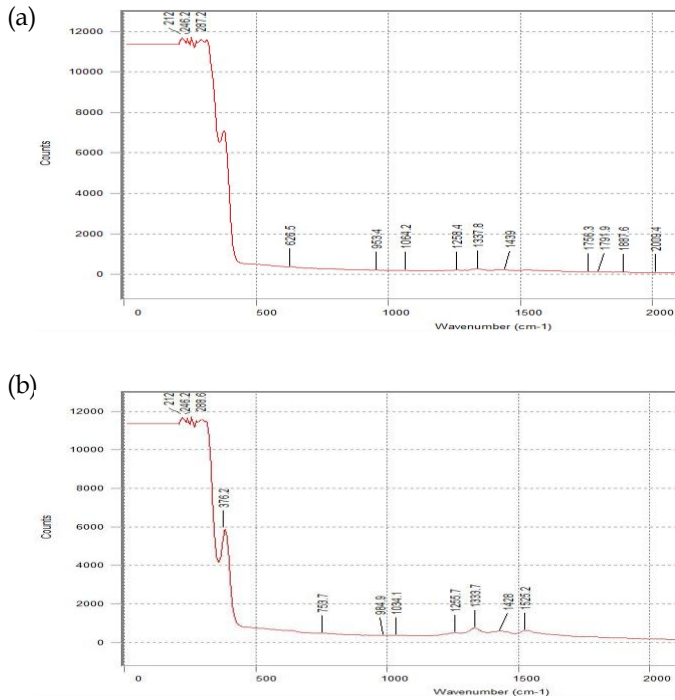


Fig.4 Raman results of 10:90 YSZ ratio on steel substrate (a) before sintering and (b) after sintering.

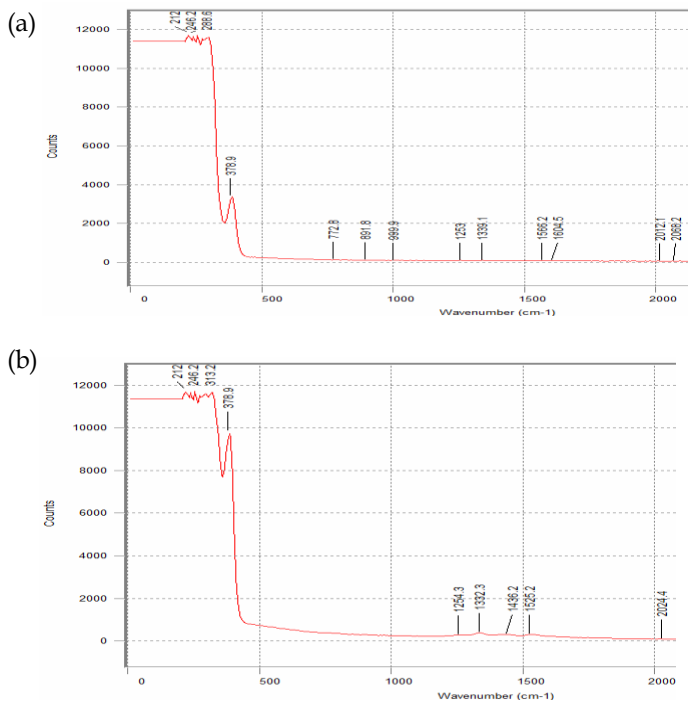


Fig.5 Raman results of 30:70 YSZ ratio on steel substrate (a) before sintering and (b) after sintering.

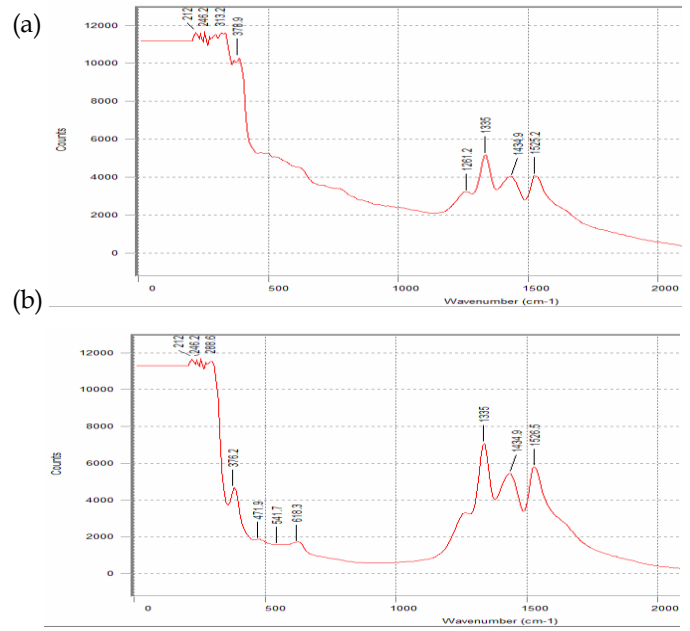


Fig.6 Raman results of 50:50 YSZ ratio on steel substrate (a) before sintering and (b) after sintering.

In Fig. 8, in terms of accumulation of material, relatively it is almost the same with the previous figure. The only difference between 30:70 YSZ films and 10:90 YSZ films is the amount of accumulation where the 30:70 YSZ film has fewer accumulation. This is because in this batch of samples, there is more YSZ in the suspension thus, making the suspension more viscous. Due to this increase of YSZ material, 30:70 YSZ films are denser compared to the 10:90 YSZ films because there is sufficient YSZ available that can cover the pores.

In Figure 9, there are no evident accumulations on the substrate. This absence of accumulation can be attributed to the density of the deposited suspension. Due to abundance of YSZ material, the 50:50 YSZ film (Figure 9(b)) became very dense and the pores are smaller compared from the other film concentration. In Figure 9(b), very few pores (pinhole like) are present.

### Cross-sectional Analysis

Figure 10(a) shows a cross sectional view of a spin coated 10:90 YSZ. It shows that making a thin film through spin coating ( $\leq 1\mu\text{m}$ ) is very possible in this concentration. But there are complications when using the 10:90 YSZ concentrations. Firstly, the film that will be created using this type of concentration is very prone to accumulation.

As shown in Figure 10(b), this is the cross sectional micrograph of a spin coated 30:70 YSZ. When using a 30:70 YSZ concentration, it is still possible to achieve a thin film ( $\leq 1\mu\text{m}$ ) through spin coating. Furthermore, the micrograph of Figure 16-17 shows that the film is almost uniform in every section of the film. This goes to show that spin coating technique is very ideal in order to produce an even thin film.

Figure 10(c) shows, the cross sectional micrographs of a spin coated 50:50 YSZ. When using a 50:50 YSZ concentration, it would be very difficult to achieve a thin film ( $\leq 1\mu\text{m}$ )

through spin coating because 50:50 concentration is very viscous. Longer spin time should be considered in order to produce thinner 50:50 YSZ film.

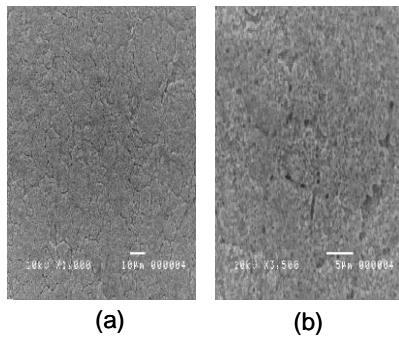


Fig. 7 SEM micrograph of sintered 10:90 YSZ ratio, spin coated on steel (a) x1,000 and (b) x3,500.

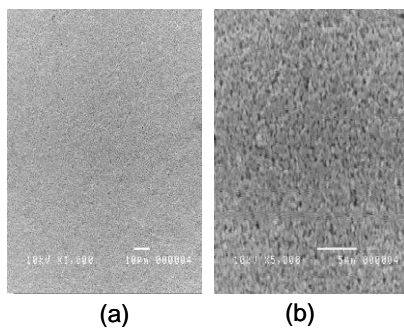


Fig. 8 SEM micrograph of sintered 30:70 YSZ ratio, spin coated on steel (a) x1,000 and (b) x3,500

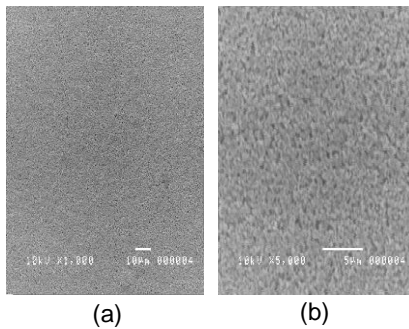


Fig.9 SEM micrograph of sintered 50:50 YSZ ratio, spin coated on steel (a) x1,000 and (b) x3,500.

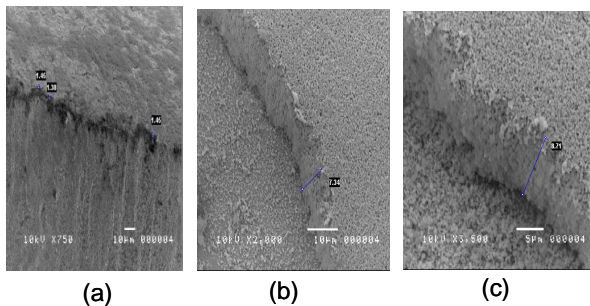


Fig.10 SEM micrographs of (a) sintered 10:90 YSZ ratio, spin coated on steel at 2500rpm for 30 seconds, (b) sintered 30:70 YSZ ratio, spin coated on steel at 2500rpm for 30 seconds, and (c) sintered 50:50 YSZ ratio, spin coated on steel at 2500rpm for 30 seconds (cross-section view).

## 4 DISCUSSION

### X-ray Diffraction

The XRD patterns revealed a cubic fluorite structure. X-ray diffraction techniques identified that the YSZ material is very stable since in every case or parameter imposed (YSZ to ethanol concentration) in the material the diffraction pattern is more likely the same. Furthermore, XRD results also showed that sintering increases the intensity of the diffraction peaks. This increase in intensity means that larger crystals are present [6].

### Raman Spectroscopy

Raman spectroscopy results further confirmed the results of the XRD that the samples have cubic fluorite structure and that the YSZ thin film did not undergo any phase change. The only changes that occurred are the increase in intensity and narrowing of the Raman peaks. This means that larger crystals were present that made the scattering more concentrated.

### Scanning Electron Microscope

The surface micrographs show that the problem of accumulation of materials that causes uneven distribution of the film can be resolved by using a higher concentration of YSZ or by using a substrate that is very smooth and even. By using a higher concentration of YSZ in a suspension, pore density can also be minimized. But as a consequence of using higher concentration of YSZ, it is expected that the film that will be fabricated will be thicker.

## REFERENCES

- [1] M. Ellis: in *Fuel Cells for Building Applications*, (New York NY: McGraw-Hill. 2002).
- [2] T. Komikado, A. Inoue, A. Takashi, & S. Umegaki: *Thin Solid Films*. **515** (2006) 3887-3892.
- [3] C. Spiegel: in *Designing and Building Fuel Cells*, (New York NY: McGraw-Hill. 2007).
- [4] K. Easler, & K. Kuan, (Eds.): in *Fuel Cell Electronics Packaging*. (New York, NY: Springer Science + Business Media. 2007).
- [5] X. Xu, C. Xia, S. Huang, & D. Peng: *Ceramics International*. **31** (2005) 1061-1064.
- [6] Y. Pan, J. H. Zhu, M. Z. Hu, & E. A. Payzant: *Surface & Coatings Technology*. **200** (2005) 1242-1247.
- [7] B. S. Yahia, L. Znaidi, & J. P. Petit: *Spectrochimica Part A*. **71** (2008) 1234-1238.
- [8] W. Tennyson. *X-ray Diffraction-The basics Followed by a Few Examples of Data Analysis*. (2007) Retrieved from [http://www.nhn.ou.edu/~bumm/NanoLab/ppt/X-ray\\_Diffraction\\_files/frame.htm](http://www.nhn.ou.edu/~bumm/NanoLab/ppt/X-ray_Diffraction_files/frame.htm) December 14, 2010
- [9] A. Gosh, A. Suri, M. Pandey, S. Thomas, T. Rama Mohan, & B. T. Rao: *Materials Letters*. **60** (2006) 1170-1173.